SOCIAL LEARNING ERRORS AND THE EVOLUTION OF MATERIAL CULTURE

LAUREN A. SCANLON[1,2], ANDREW LOBB[1], JAMSHID J. TEHRANI[2], JEREMY R. KENDAL[2]
[1]DEPARTMENT OF MATHEMATICS, DURHAM UNIVERSITY
[2]DEPARTMENT OF ANTHROPOLOGY AND CENTRE FOR THE COEVOLUTION OF BIOLOGY AND CULTURE, DURHAM UNIVERSITY

Abstract. Research into the evolution of material culture has focused on cognitive capacities that enable innovation and the high fidelity transmission of complex knowledge and skills between individuals and across generations. However, the causes and consequences of copying error remain relatively poorly understood. Our case study concerns the ancient and ubiquitous technology of knot tying, focusing on simple variants in microstructure formed by the composition of two trefoil knots. We apply a mathematical model to experimental data to make quantitative estimates from three classes of cognitive factors that can affect the production of cultural variation during the process of social learning. Despite a relatively high fidelity of copying or imitation, we also find evidence for an absolute learning bias towards an un-observed cultural variant (handedness), a relative transformation of the observed cultural variant (mirroring), and a propensity to repeat previously performed chunk of behaviour in a sequence. Our analysis shows how these cognitive factors interact to affect cultural evolutionary dynamics and that even in the absence of non-random errors, their interactions result in a non-random distribution of cultural variation. We discuss how parameterisation of cognitive factors involved in social learning can be used to assess their effects on the unintended production of cultural variation and evolutionary dynamics.

1. Introduction

High fidelity social learning and innovation are considered crucial processes underpinning cumulative cultural evolution, enabling individuals to acquire and modify knowledge that exceeds that which any single individual could invent alone [1] [2]. However, social learning is not usually perfect [3]; copying errors may affect the fidelity of transmission, causing the accumulation of copying error observed in material culture [4].

It is plausible that most social learning errors are non-random, biased by anatomical, cognitive and environmental features [5]. For example, experimental evidence suggests that 'reductive' mutation of an artefact results in greater population-level variation than 'additive' mutation [7], and that perceptual bias of whether an object must be increased or decreased in size to match a model object size can result in a respective decrease or increase in the population mean size over simulated generations [6]. Also, learners attempting to imitate can perform the mirror image of a demonstrated action [8] [9] because they are vulnerable to the correspondence problem, which requires mapping between the perspective of the demonstrator and the observer [10]. This can be particularly challenging when these perspectives differ, that is they are perpetually opaque [11]. Some social learning errors can result from embodied cognition through interaction of the brain and anatomical features. For instance, cultural and genetic propensity for a cognitive bias towards right-handedness has interacted with the asymmetric position of the hand's opposable thumb to affect a wide range of technology, including cooking and writing implements, construction tools and musical instruments. Social learning biases have also been shown to affect cultural evolution in domains besides technology, including language [12], art [13] and narrative [14].

Following seminal works by Cavalli-Sforza and Feldman, and Boyd and Richerson [15] [16], models of within-population cultural evolutionary dynamics typically parameterise the effects of mutation, transmission and selection but neglect the effects of non-random error during social learning as a source of cultural variation [16][3]. Typically, cultural variation is assumed to result from random mutation or directed individual modification following, but not during, the process of social transmission, called 'guided variation' [3]. Cultural variants are subject to selection via differential adoption of a trait based on: characteristics of the model demonstrating the variant (e.g. a preference to copy a successful individual); the frequency of the variant (e.g. a preference to copy a popular variant); or an intrinsic preference for the variant (e.g. a preference to learn, recall and transmit social over technical information). These selective processes alter the relative frequencies of extant variants but are not sources of variation.

A distinct approach to modelling cultural evolution, called cultural attraction theory, highlights 'factors-of-attraction' as non-random causes of change in cultural variant frequencies, including cognitive factors affecting the construction of

information during the social learning process [17][18]. Claidiere et al. [5] formalize this approach using a parameter-free model where the linear effect of a transition matrix is used to predict the change in frequency of cultural variants between generations and includes the combined effects of any factors-of-attraction.

Our study draws upon both approaches by developing a parametric model of within-population cultural evolutionary dynamics to explore the combined effects of the three classes of cognitive factors which may affect the production of cultural variation during social transmission. First, variation may be caused by an (absolute) learning bias towards an un-observed cultural variant; for instance, a learner may observe a left-handed technique but adopt the right-handed equivalent form. Second, a learner may generate a new variant by adopting a consistent (relative) transformation of the observed cultural variant; for instance, by adopting the mirror image of what they observed. Finally, when a behavioural sequence, or chaine-operatoire, is learned in chunks [19][**?**], a propensity to repeat previous chunks, or not, can affect sequence variation measured across the population.

As a case study, we consider the social transmission of micro-structures in knot tying, focusing on variation in the composition of two trefoil knots, known commonly as granny and reef knots. Originating 300kbp [20] and preserved from 5500 bp [21], simple knots are an ancient technology and remain relatively ubiquitous [22]. The simplest knot, the trefoil or overhand knot, can take either a left (L) or right (R) handed form, and the composite of two such trefoils are both granny knots, formed of two left- or two right-handed trefoils (LL or RR), or reef knots, formed of a left- and a right-handed trefoil (LR or RL) (Figure 1a). These knots are typically used to tie shoelaces, by forming an overhand knot and then forming a slipped overhand knot on top.

Shoelaces are commonly tied using a granny knot and, more generally, analysis of the Ashley Book of Knots [22] revealed that from the composition of two trefoils, the granny knot appears in 75% of cases (reef in 25%) [23]. An analysis of impact in integrity of knot structure shows that the reef knot is less liable to come undone, suggesting that non-functional biases may be required to explain the prevalence of the granny [24][25].

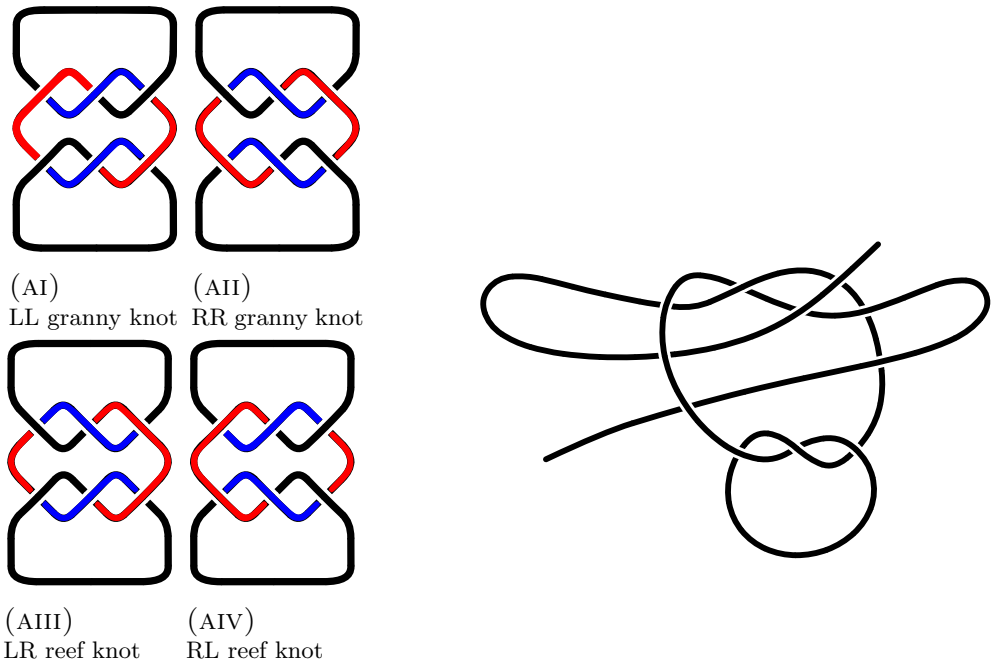

(A) Mathematical knots (B) Shoelace knot

FIGURE 1. Figure 1a shows all possible mathematical granny and reef knots. Figure 1b illustrates a shoelace knot tied using a RL reef knot.

Mathematically, a knot is a 3-dimensional closed curve, where the string is over and under itself in some way with the ends glued together. The left- and right-handed versions of the trefoil are mirror images of one another and are mathematically distinct as they cannot be transformed into each other by Reidemeister moves [26] (a set of moves on the strands of a knot used to determine if two diagrams relate to the same knot); the only way to change the left handed trefoil to the right handed trefoil is to cut the knot open and retie it. The granny and reef knots are distinct knots, and can be identified as such by knot invariants [27]. Knot invariants will give the same result when two knots are the same, and different results when they are distinct. The Jones polynomial [28] is one such invariant, which assigns a polynomial to each knot and gives us some information about the crossings of that knot. The Jones polynomial is given for the left handed granny knot in Equation 1, the right handed granny knot in Equation 2 and both reef knots by Equation 3. We can see that the Jones polynomial for the left handed granny knot differs right handed granny knot by the sign of the exponents in the polynomial, the exponents for the left handed granny knot are all negative whilst they are positive for the right handed granny knot. This is the only difference

between the two polynomials and shows that the left handed and right handed granny knot are mirror images of one another. Both versions of the reef knot have the same Jones polynomial which contains both positive and negative values for the exponents showing that there is no difference between the two versions of this knot. These polynomials show that the granny knots are distinct from each other and both reef knots, but the two reef knots are not distinct, which can be seen by rotating one reef knot to match the other; no such rotation is possible for the granny knots (See Figure 1a).

$$V_{LL}(t) = t^{-2} + 2t^{-4} - 2t^{-5} + t^{-6} - 2t^{-7} + t^{-8} \tag{1}$$

$$V_{RR}(t) = t^{2} + 2t^{4} - 2t^{5} + t^{6} - 2t^{7} + t^{8} \tag{2}$$

$$V_{reef}(t) = -t^{3} + t^{2} - t + 3 - t^{-1} + t^{-2} - t^{-3} \tag{3}$$

We apply experimental and modelling approaches to identify evidence for non-random error affecting the social transmission of all forms of granny (LL, RR) and reef knot (LR, RL). We use the models to predict their effects on the evolution of knot diversity in this closed system.

2. Social Transmission Experiment

The experiment consisted of two stages. The first stage established trefoil handedness bias among participants in the absence of a social demonstration. The second stage established social transmission fidelity of the granny and reef knots (LL, RR, LR and RL). Participants were recruited from the student population of Durham University. They were rewarded with a £4 food voucher for their participation. In total 101 people took part in the experiment with 36 male. The experiment took place in a lecture theatre, with batches of up to 10 participants at a time. We treated between-participant effects as independent by spacing participants widely across the lecture theatre and requiring each participant to tie their knots within a modified cardboard box which prevented between-participant observation.

2.0.1. *Stage 1.* We asked participants to tie a "simple knot". We then checked that this was a trefoil knot. The knot was undone, then participants were asked to tie a "simple knot" every 60s over a 10 minute period. Each knot was tied in a separate 25cm length of string and the sealed in a small plastic bag. Over the same period, participants were asked to complete a distraction task in between tying each knot, requiring them to draw six concepts in order that another person could match the concepts to the drawings at a later time. Both the plastic bag containing the 10 knots and the paper with the drawings from the distraction task were collected in at the end of this stage.

2.0.2. *Stage 2.* Participants were given 35cm length of string and shown a video demonstrating the tying of either a LL granny knot (26 participants), a RR granny knot (25 participants), a LR reef knot (25 participants) or a RL reef knot (25 participants), randomly assigned across batches (screenshots of the video and the knots are shown in Figure 2). The video showed only hands tying a knot and contained no audio. The video was recorded from the point of view of an observer sitting across from the demonstrator. Participants were shown the video three times, with a pause of 30 seconds between each showing. They were told they could practice tying the knot whilst the video was being shown, and during the pauses between the showings. After the final showing of the video, they were told to untie any practice knots and asked to retie the knot shown in the video. This delay effect was to reflect the process of learning from a demonstration.

2.0.3. *Questionnaire.* After both stages had been completed and all material collected, participants were asked to complete a short questionnaire detailing their name, gender, degree programme, handedness, hand usually used for writing, their knot tying experience and whether they knew how to tie a granny or reef knot. Details of the responses from the questionnaire can be found in Appendix A.

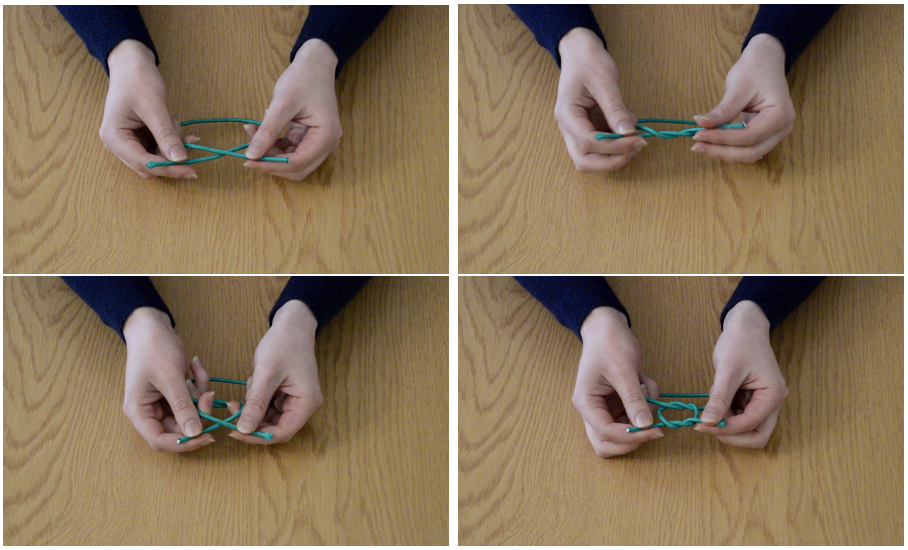

(A) Screenshots from video showing the tying of RR granny knot

(BI) LL granny knot

(BII) RR granny knot

(BIII) LR reef knot

(BIV) RL reef knot

(B) Tied granny and reef knots

FIGURE 2. Screenshots from a demonstration video used in the experiment and tied versions of all four knots used.

2.1. **Results.** For each participant in stage 1, we recorded knot handedness over the 10 trefoils as an estimate of knot handedness bias in the absence of a demonstration. The frequency of right handed trefoils tied by each person is shown in Figure 3, where participants who tied no right handed trefoils tied all left handed trefoils. Two participants who tied knots which were not trefoils have not been included in these data.

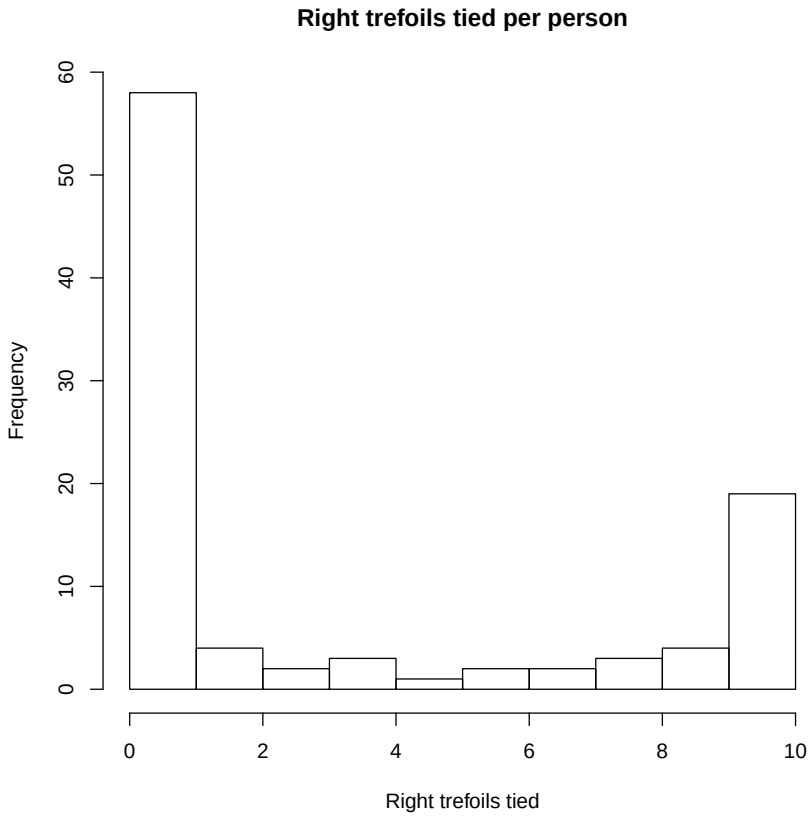

FIGURE 3. Frequency of right handed trefoils tied by participants, those who tied no right handed tied all left handed trefoils and vice versa

The majority of participants tied either all right handed or all left handed trefoils, with a few tying a mixture of the two. Left handed trefoils were much more common than right handed trefoils. The mean proportion of right handed trefoils tied per person was 0.32. A Bayesian association analysis (see Figure 12) revealed weak evidence that individuals who typically write with their right hand are more

likely to tie a left-handed trefoil than those write with their left, while those using their left hand to write are more likely to tie a right-handed trefoil than those who use their right.

Of the 101 knots tied after being shown the video, 100 of the knots were either LL, RR, LR or RL, and the remaining knot (a composition of the knot 5_1 and the knot 3_1) was excluded from the analysis.

		Knot tied by participants				
		LL	RR	LR	RL	Total
Demonstration	LL	14	9	1	2	26
	RR	9	15	0	1	25
	LR	4	4	8	8	24
	RL	6	1	6	12	25
	Total	33	29	15	23	100

TABLE 1. Knots tied by participants given video shown in experiment, dashed lines delineate granny knots from reef knots

		Stage 2 knots tied by participants				
		LL	RR	LR	RL	Total
Stage 1 handedness bias	Left	25	20	12	11	68
	Right	6	9	2	12	29
	Total	31	29	14	23	97

TABLE 2. Knot tied given handedness of trefoil tied by participants, dashed lines delineate granny knots from reef knots

Table 1 and Bayesian posterior distributions (see Appendix B, Figures -) for the probability of tying a knot given the knot shown both show that participants were most likely to tie the knot shown in the video, but that if a mistake was made, participants were most likely to tie the mirror image of the demonstrated knot over the other two variants. For example, more people tied the RR granny knot when shown LL, than tied either reef knot, LR or RL. Table 1 and Bayesian posterior distributions also indicate that granny knots were more likely to be tied than reef knots, suggesting that participants may exhibit a bias to repeat the handedness of the first trefoil they tie. Finally, participants that exhibited a handedness bias in stage 1, displayed the same bias in the first trefoil tied following the demonstration in stage 2, suggesting that knot handedness bias may affect social transmission

fidelity. For example, those who had a left-handed bias in stage 1 were more likely to begin their post-demonstration knot with L than R (see Appendix B Figure 17).

Having identified preliminary evidence for imitation of the demonstrated knot, knot-handedness bias, mirroring and repetition, we develop a model that explores their effects on cultural evolutionary dynamics. We use the model to estimate their effect size in the experiment and consider the evolutionary trajectories that might result if experimental social transmission was iterated over many generations. We contrast the predictions of this parametric approach with those of a non-parametric approach where transmission dynamics are determined by a transition matrix calculated directly from the social transmission experimental data.

3. Social Transmission Model

3.1. **Assumptions.** We model the transmission of granny and reef knots within a population through oblique transmission [15] and assume a closed system such that when a granny or reef knot is demonstrated, the learned knot is always either a granny or a reef knot. Following the results of the experiment, we assume that four parameters can affect the fidelity of social transmission: the learner interprets the demonstrator's knot incorrectly as the knot's mirror image with a probability g; the learner imitates each perceived form of trefoil with a probability s, where the perceived knot refers to the learner's interpretation of the demonstrated knot, which could either be the demonstrated knot or the mirror image of the demonstrated knot; the learner repeats the trefoil they tied for the first step of the knot with a probability r; and the learner ties a right handed trefoil when they do not learn from the demonstration with a probability p.

Using these parameters, we can build a system of recurrence equations to describe knot frequencies in the learner generation as a function of knot frequency in the demonstrator generation. We denote the proportion of knot ij tied in the demonstrating generation by f_{ij} where $ij \in \{RR, LL, RL, LR\}$, and the knots tied by the learner generation of the population after transmission as f'_{ij} where $f'_{RR} + f'_{LL} + f'_{RL} + f'_{LR} = 1$ with each f'_{ij} taking values in the interval $[0, 1]$. For example, take the granny knot formed by tying two right handed trefoils and denote it by f_{RR}. This knot will be transmitted successfully if it is not mirrored and both trefoils that form it are accurately imitated by the next generation, denoted by $f_{RR}(s^2(1-g))$. However, a right granny could also be formed by mirroring an LL with probability g and accurately imitating both trefoils of the perceived knot with probability s^2, giving $f_{LL}(s^2 g)$. A right granny could also be formed with no imitation at all, if the tyer has a bias towards tying right handed trefoils $f_{RR}((1-s)^2 p^2)$ or repeating the first knot tied, $f_{RR}((1-s)^2(pr))$ and so we get the frequency of right grannies in the population as a function of grannies and reefs

already in the population and the probability parameters;

$$f'_{RR} = f_{RR}(s^2(1-g)) + \cdots + f_{RR}((1-s)^2p^2) + \ldots \\ + f_{RR}((1-s)^2(pr)) + \cdots + f_{LL}(s^2g) + \ldots \tag{4}$$

It is important to think about how the parameters interact with each other. If a learner imitates the knot correctly then the learner's likelihood to repeat or tie a right handed trefoil does not matter. They will do what is shown regardless of their biases, and so we can discount repetition and right hand bias when the knot is accurately imitated. In the same way, when the learner simply repeats part of a knot their right hand bias does not matter, as they will repeat regardless of this bias. So we can discount right-hand bias when repetition takes place. Figure 4 illustrates the effect of parameters on the transmission of knot RR in the order of mirroring, accuracy, repetition then handedness bias, but the order does not actually matter as the parameters commute and will cancel with each other (see Appendix C, for the recursions for all four knots).

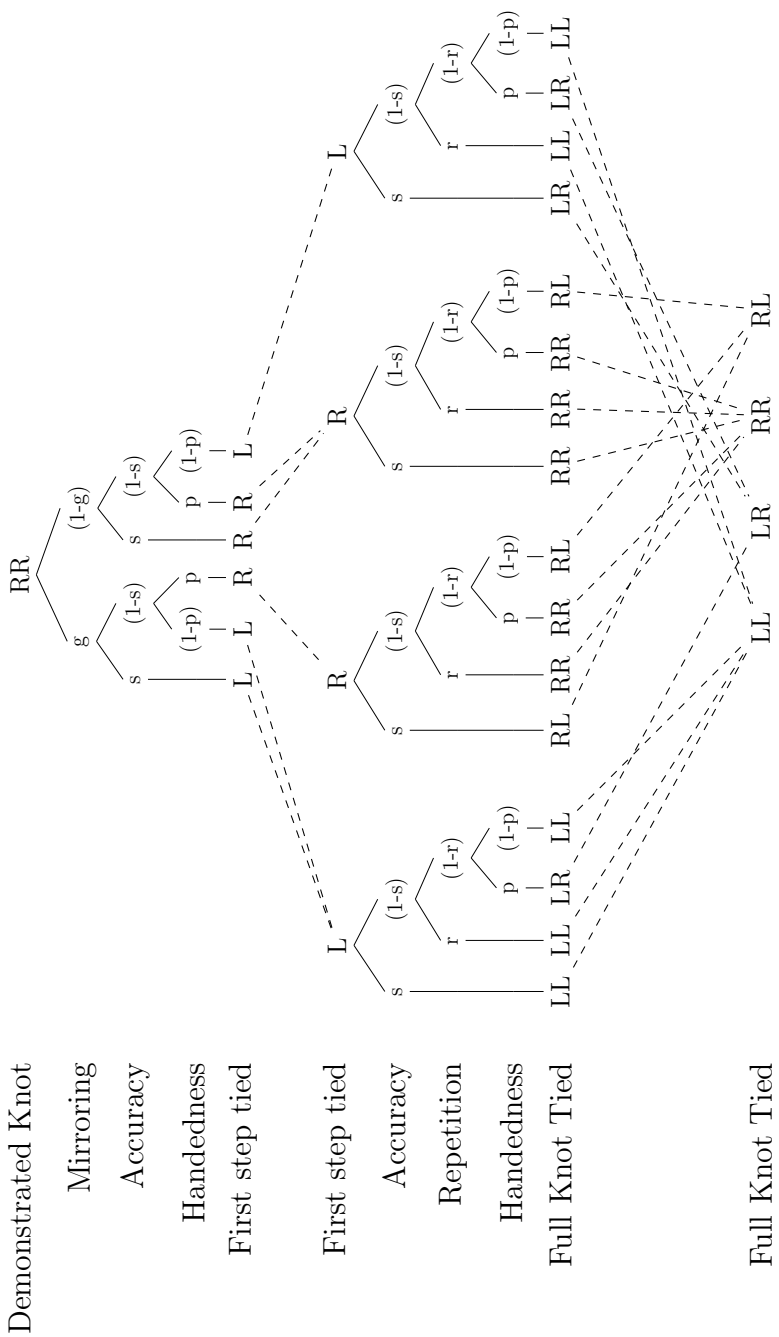

FIGURE 4. Decision tree showing the effect of parameters on the transmission of knot RR

3.2. **Evolutionary Dynamics.** Each set of parameter values $0 \leq (s, g, r, p) \leq 1$, determines the evolutionary trajectory and a single equilibrium point, where $f_{ij} = f'_{ij} = \hat{f}_{ij}$, (expressions for equilibrium states are given in Appendix D). If $s = 0$, the system jumps to a stable equilibrium point determined by the p and r and is unaffected by starting values of f_{ij}. By contrast, if imitation is always accurate, $s = 1$, and mirroring never occurs, $g = 0$ $(0 \leq r \leq 1)$, the population does not evolve from starting frequencies, so if a small perturbation in frequencies is induced, the population remains at the new frequencies. If there is some imitation, $0 < s < 1$, the population evolves to a stable equilibrium, such that the population returns to the original equilibrium state following a small perturbation in frequencies.

Figure 5 illustrates the effect of imitation accuracy and mirroring on equilibrium frequencies. In Figure 5a, the value of s is set lower than in 5b, resulting in only a slight change in the values of $\hat{f}_{RR}$, $\hat{f}_{LL}$ and $\hat{f}_{RL}$ and $\hat{f}_{LR}$. This is compared with the higher value of s in 5b and the curved lines representing the frequencies. This shows that imitation needs to be highly probable for mirroring to affect the proportion of knots tied in the population. We notice that the two reef knot frequencies, f_{LR} and f_{RL}, are always equal at equilibria. This is consistent with the fact that LR and RL represent the same knot mathematically, as shown by their Jones polynomial in Equation 3.

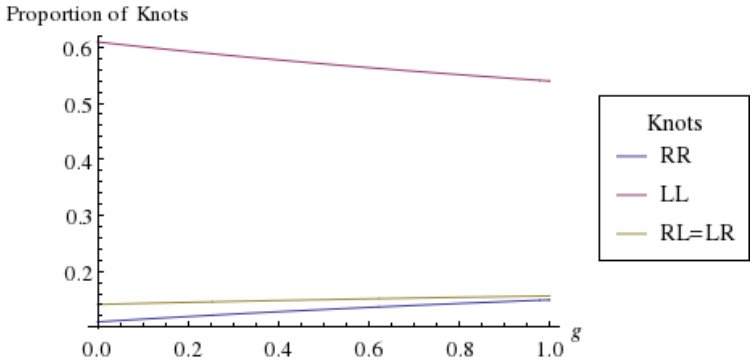

(A) p=0.25, r=0.25, s=0.1

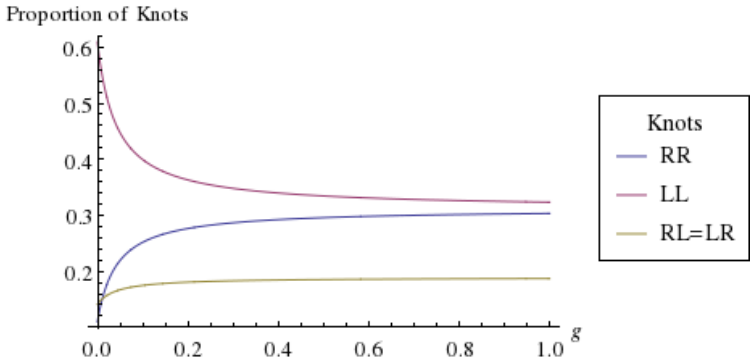

(B) p=0.25, r=0.25, s=0.9

FIGURE 5. Line plots showing the proportion of knots at equilibria when the imitation coefficient is (A) low, and (B) high. The values of $\hat{f}_{LR}$ and $\hat{f}_{RL}$ are equal so these are represented by the same line on the graph, while $\hat{f}_{RR}$ and $\hat{f}_{LL}$ are represented by separate lines.

Prior to reaching an equilibrium state, evolutionary dynamics typically follow a smooth trajectory (assuming $0 < s < 1$), but a high probability of mirroring can cause oscillations in the trajectory when imitation accuracy is high. When mirroring is low (Figure 6a), we see the system evolve in a smooth curve to a point strongly affected by the handedness bias, p and repetition bias, r. The value of p causes the point to be closer to the corner f_{RR} than f_{LL} but the value of r does not cause the point to be as close to the $f_{RL} + f_{LR} = 1$ boundary as we may expect. In 6b, mirroring is likely to occur. Coupled with the high imitation accuracy, the system evolves to a similar equilibrium point as shown in 6a, but the high probability of mirroring causes the path to oscillate to the point rather than evolve in a smooth trajectory.

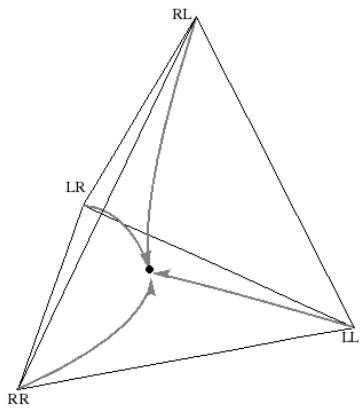

(A) p=0.75,g=0.1,r=0.25,s=0.9

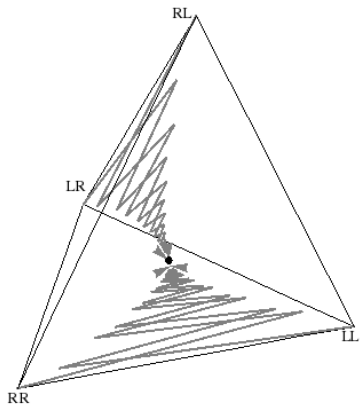

(B) p=0.75,g=0.9,r=0.25,s=0.9

FIGURE 6. Evolutionary plots showing the change in frequency of knots. Each arrow represents the change in frequency of each type of knot in the population, starting from sole existence in each corner to a mixture of different knots. The solid disk is the equilibrium state which is evolved towards no matter the starting frequencies. Frequencies are plotted in tetrahedral space using barycentric coordinates (see Appendix F).

Most combinations of parameter values result in an excess of granny knots over reef knots at equilibrium. As noted above, any repetition bias will favour the granny knot, but even when repetition never occurs, the population is still more likely to tie granny knots than reef knots if there is any handedness bias. Figure 7 illustrates the predominance of granny knots at equilibrium, taking the case where there is no repetition in the absence of guidance, $r = 0$, and intermediate mirroring, $g = 1/2$. The bias towards granny knots is strongest when handedness

bias, p, is either high or low and the imitation coefficient, s, is low; in other words, when individuals consistently tie with the same handedness rather than imitating a different knot.

There are only two cases where the equilibrium proportion of granny and reef knots is equal ($\hat{f}_{RR} + \hat{f}_{LL} = \hat{f}_{RL} + \hat{f}_{LR}$). The first case is when imitation is not perfect, $0 \leq s < 1$, the first knot is never repeated, $r = 0$, and there is no handedness bias, $p = 1/2$, where $0 \leq g \leq 1$. The absence of repetition bias prevents predominance of granny knots, and the lack of handedness bias prevents the prevalence of either granny knot. The second case is when imitation always occurs, $s = 1$, individuals never repeat the first knot tied, $r = 0$, and there is some mirroring $0 < g \leq 1$, where $0 \leq p \leq 1$. Again, the absence of repetition bias prevents predominance of granny knots, *perceived* imitation is always perfect, but mirroring causes knots to be copied incorrectly. Both these cases are illustrated in Figure 7. Finally, we note that reef knots can only be more prevalent than granny knots if this is exhibited in their starting frequencies and when the system does not evolve ($s = 1$ and $g = 0$; discussed above).

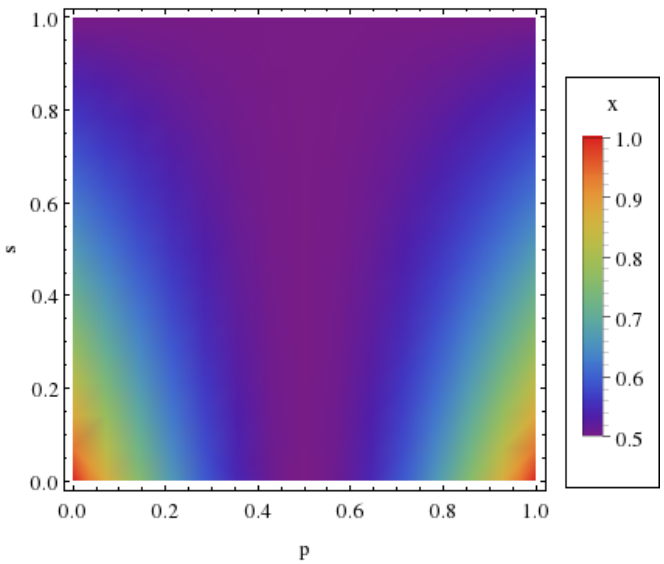

FIGURE 7. Density plots showing the proportion of granny knots at equilibrium, denoted by $x = \hat{f}_{RR} + \hat{f}_{LL}$, as a function of the handedness-bias, p and the imitation coefficient, s, where g=1/2 and r=0.

4. Applying the Parametric model to Experimental Results

Using Approximate Bayesian Computation (ABC) [29], we can use our model to estimate parameter values that predict the experimental data. ABC works on the same premise as Bayes' theorem, relating conditional probability of parameters θ, to data D by the rule

$$p(\theta|D) = \frac{p(D|\theta)p(\theta)}{p(D)}, \tag{5}$$

where $p(\theta|D)$ is referred to as the posterior, $p(\theta)$ represents the prior beliefs before any data is available, $p(D|\theta)$ the likelihood of data D occurring given the prior and $p(D)$ the evidence [30]. With this rule, we can calculate the posterior by taking the product of prior beliefs with the likelihood of data occurring, divided by the evidence observed. To obtain the probability of data D given parameter θ, we use our model to simulate data for a given parameter set and decide whether it fits the observed data. We construct a metric to describe our observed data such that we can accept or reject the simulated parameter set depending on whether it generated data within a tolerated degree of proximity from the observed. The retained parameter distributions give us $p(\theta|D)$.

Taking our observed data from Table 1 as a 4×4 matrix O and simulating data of the same form using our model to give a 4×4 matrix S, we compare these two sets of data using the metric;

$$d(O, S) = \sum_{i,j} a_{ij}^2, \tag{6}$$

where a_{ij} are the entries of the matrix $O - S$. This metric is proportional to finding the Euclidean distance between the points in the two matrices.

We use grid approximation and simulate data for values of each parameter p, g, r and s between 0 and 1 with intervals of 0.01. The simulations match the experimental conditions by starting with even frequency states, $f_{ij} = 1/4$, and running the simulation over a single generation. The metric in Equation 6 is calculated for all 101^4 simulations.

4.1. ABC results.

Figure 8 shows the parameter distributions from the 204 simulations that resulted in a metric value, $d(O, S) = \sum_{i,j} a_{ij}^2 \leq 0.04$. We see from these plots that the value of the parameters can almost be stated explicitly. Taking the mean value at 2 decimal places for each parameter, which is equal to the median and the mode, we note a non-random, right-handed trefoil bias ($\bar{p} = 0.35$), predicting that more left handed trefoil knots are tied by the population when given no guidance than right handed trefoils. This value is similar to our experimental (stage 1) mean handedness bias, 0.32. The model predicts that individuals mirror fairly frequently ($\bar{g} = 0.39$) but that knots are mirrored less often than they are correctly interpreted. Also, individuals are more likely to repeat the first part of the knot tied than not ($\bar{r} = 0.61$). Finally, there is a relatively high accuracy of

imitation ($\bar{s} = 0.79$). These results are concordant with our interpretation of the descriptive statistics from the experiment (see Table 1).

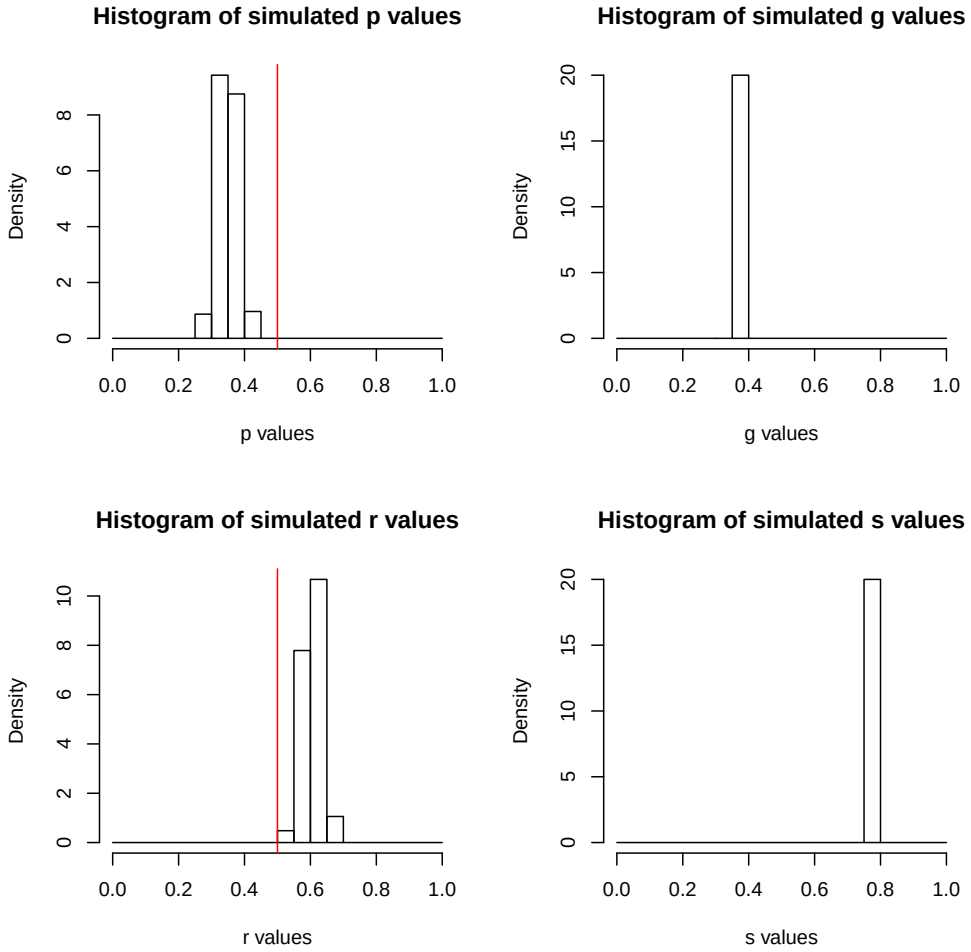

FIGURE 8. Histograms of parameter values from the the 204 simulations retained within acceptance interval $d(O, S) \leq 0.04$. Red lines indicate unbiased parameter values, $p = 1/2$ and $r = 1/2$, giving equal probability of tying right- and left-handed trefoils and equal probability of repeating the previous knot as not, respectively.

We can establish what effect our posterior parameter estimates would have on the cultural evolution of granny and reef knots by plugging these values into the model. Figure 9 shows how the population evolves towards a single polymorphic equilibrium state, no matter the starting distribution (grey arrows leading to black disc). The effect of the high posterior imitation value, $\bar{s} = 0.79$, is shown by

comparing this equilibrium state against the expected equilibrium frequencies in the absence of social learning ($s = 0$, red disc).

We can see the effect of learning biases by comparing against trajectories where these biases are absent ($p = 0.5, r = 0.5, g = 0$; blue arrows leading to blue disc). Although imitation is a relatively high value, $\bar{s} = 0.79$, granny knots evolve to be more common than reef knots, caused by the repetition bias, while left-handed granny knots are more common than right, caused by the handedness bias. Given the high posterior mean imitation value, the posterior mean mirroring value is not large enough to cause the characteristic oscillating dynamics shown in Figure 6b and has negligible effect on the relative equilibrium frequency of left- to right-handed granny knots.

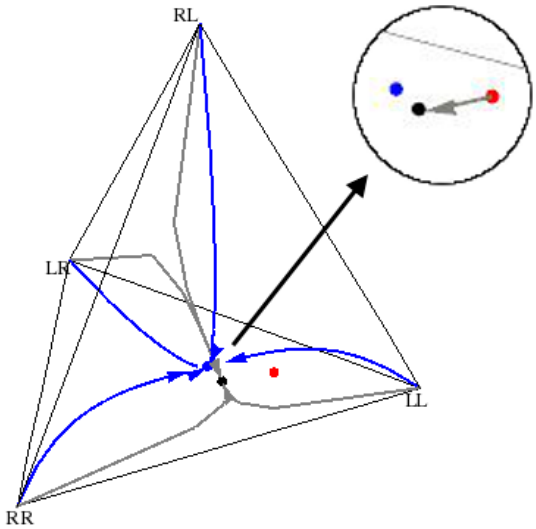

FIGURE 9. Evolutionary trajectories of the four knot forms, where $f_{ij} = 1$ in each corner and frequencies are equal at the centre of the tetrahedron, plotted by converting frequencies to Barycentric coordinates. Trajectories using the mean posterior parameter values are shown by the grey arrows and black disc, $\hat{f}_{LL} = 0.4241, \hat{f}_{RR} = 0.3835, \hat{f}_{LR} = \hat{f}_{RL} = 0.0962$. In the absence of social learning, the expected knot frequencies are shown by the red disc $\hat{f}_{LL} = 0.5613, \hat{f}_{RR} = 0.2613, \hat{f}_{LR} = \hat{f}_{RL} = 0.0887$, and are governed by the degree of repetition and handedness. The blue arrows and disc, $\hat{f}_{LL} = 0.375, \hat{f}_{RR} = 0.375, \hat{f}_{LR} = \hat{f}_{RL} = 0.125$, show the trajectories in the absence of learning biases and mirroring, $p = 0.5, r = 0.5, g = 0$, where $\bar{s} = 0.79$.

Finally, we note that the absence of learning biases does not necessarily lead to equal knot frequencies of cultural variants (i.e. the blue disc is not in the centre of the tetrahedron), rather that granny knots are expected in higher frequency than reef knots. This occurs because of the non-independent relationships between the parameters. Consider for instance the case where there is no social learning in the absence of both handedness or repetition biases and mirroring $p = 0.5, r = 0.5, g = 0, s = 0$. Figure 10 shows that the probability of tying each knot is $P(LL) = \frac{3}{8}$ and $P(RR) = \frac{3}{8}$, and $P(RL) = \frac{1}{8}$ and $P(LR) = \frac{1}{8}$.

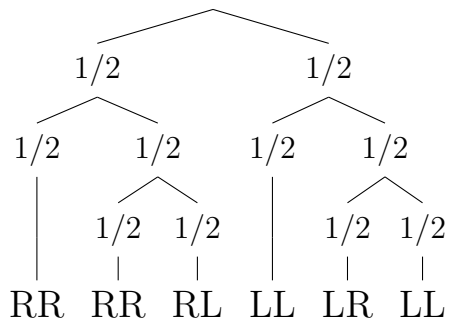

FIGURE 10. A decision tree showing knots tied in the absence of biases in handedness ($p = 0.5$; top layer decision) and repetition biases ($r = 0.5$; second layer decision).

4.2. **Comparing Parametric and Non-parametric Approaches.** We compare the equilibrium results of the parametric model, described above, with a non-parametric approach which predicts equilibrium frequencies from the transmission matrix which is taken directly from the experimental data (Table 1), and represents the probability of the change in knot types from those demonstrated to those learned. For example $x_{2,1} = P(LL|RR)$ is the probability of tying knot LL when shown RR.

$$X = \begin{bmatrix} \frac{14}{26} & \frac{9}{26} & \frac{1}{26} & \frac{2}{26} \\ \frac{9}{25} & \frac{15}{25} & 0 & \frac{1}{25} \\ \frac{4}{24} & \frac{4}{24} & \frac{8}{24} & \frac{8}{24} \\ \frac{6}{25} & \frac{1}{25} & \frac{6}{25} & \frac{12}{25} \end{bmatrix} \tag{7}$$

X is a right stochastic matrix representing the frequency of change in knots tied given by the experimental data. We can simulate social transmission of these knots within future generations by taking powers of this matrix, basing future generations solely on the present state. This approach treats any cognitive factors affecting change in cultural variant frequency as implicit, linear effects in the

transition matrix. After 20 generations we have stability in transmission such that the probability of tying any given knot remains constant (measured to 3 decimal places).

Knot	Parametric Approach	Non-parametric Approach
LL	42.41%	40.1%
RR	38.35%	39.1%
LR	9.62%	7.2%
RL	9.62%	13.6%

TABLE 3. Percentage of each type of knot in the population at equilibria, calculated using the parametric and non-parametric models.

Table 3 shows that both the parametric and non-parametric models predict a prevalence of granny over reef knots at equilibrium, but the parametric approach predicts a higher left- to right-handed bias in granny knots and, unlike the non-parametric approach, gives equal frequencies of both reef knots. The non-parametric approach makes no theoretical assumptions over how cognitive factors interact so it is unsurprising to find unequal reef knot frequencies. The parametric model behaviour is, by definition, determined by the probabilistic interactions of proposed cognitive factors (s, g, r, p) but the model does not assume that individuals recognise or treat the two reef knots to be mathematically the same.

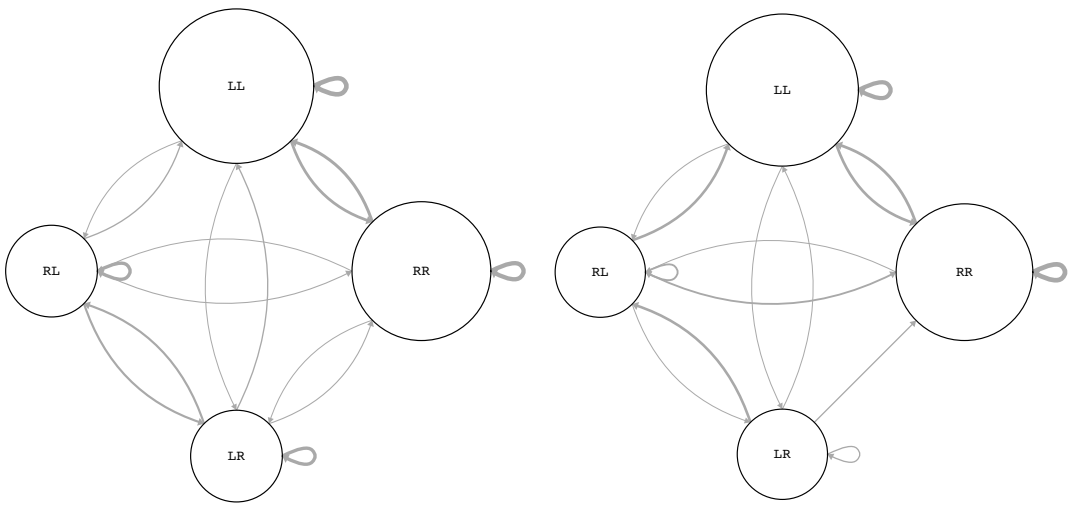

(A) Parametric Model (B) Non-parametric model

FIGURE 11. Weighted graph demonstrating the transmission of each knot under (A) a parametric approach and (B) a non-parametric approach

Figure 11b shows the transmission of each knot type from the transition matrix. We observe the absence of knot transitions from RR to LR as none did so in the experimental data. Occurrences like this lack of transition can affect the expected equilibria under the non-parametric approach, causing lower frequencies of knot LR to be expected, as seen in Table 3 but are not seen under the parametric approach shown in Figure 11a.

5. Discussion

In this paper we have combined an experiment and model to investigate the effects of non-random learning errors on the evolution of granny and reef knots. Using experimental data we have seen that granny knots are more commonly correctly transmitted than reef knots. Using ABC, we predict that participants in the experiment were less likely to mirror than not to mirror the demonstrated knot but likely to imitate the perceived knot. Also, on average, they were biased towards tying left handed trefoils and more likely than not to inadvertently repeat the first knot tied.

The estimate of mirroring suggests that faithful cultural transmission is vulnerable to the correspondence problem [11] in which case this effect might be reduced if observers and demonstrators sit side-by-side, taking a similar visual perspective. The average bias towards left-handed knots may be a relatively asocial phenomenon as this was observed in both the asocial stage (1) and demonstration state (2), and was strongly correlated with the handedness of the individual. While complex skills can be honed by repetition, our study suggests that a tendency for inadvertent repetition of task chunks can reduce within-sequence variation over evolutionary time, in this case promoting granny over reef knots.

Our results suggest that errors in attempts to faithfully reproduce demonstrated knots are unlikely to be random, and can affect cultural evolutionary trajectories even when transmission fidelity is relatively high, as the population evolves towards an equilibrium characterised by a prevalence of left- over right-handed granny knots and a preponderance of granny knots over reef knots. Even if the proposed cognitive factors were unbiased in their effects, their interactions do not produce an even distribution of knot forms because of their conditional, or nested, effects. Thus empirical evidence for granny over reef knots does not necessary result from a knot preference (although it may) but from the interaction of cognitive factors that affect their construction.

We contrast the equilibrium states that result from the parametric and non-parametric approaches and note that only the parametric model predicts equal frequencies of the two reef knot frequencies. While there is no assumption in the model that individuals recognise both forms of reef knot to be equivalent, the proposed cognitive factors result in an equilibrium state that is consistent with our mathematical understanding that these two forms (LR and RL) are actually the same knot. This result is caused (in an evolving population) by any degree of

imperfect imitation (i.e. $0 \leq s \leq 1$), which increases variation in cultural forms by driving the population toward equal frequencies of all knot forms; this only holds where individuals tie some form of trefoil knot, rather than abstaining from the knot-tying behaviour if they fail to imitate. Mirroring also pushes the population toward equal frequencies of knot forms because it is most likely, by chance, to reverse the handedness of the most common trefoil. Thus the effect of these two factors accounts for the parity of reef knot forms at equilibrium but, on their own, would also have a similar effect on forms of granny knot, even though these are not mathematically identical. The parity of reef knot forms at equilibrium should not be used as confirmation of a 'good' model; rather, cognitive factors act in a way that results in variation that is consistent with mathematical classification of knots.

Cladiere et al. ([5], p.5, Table 1 and Eq.4.1) use a non-parametric transition matrix, which they label an "evolutionary causal matrix" (p.5), to illustrate evolutionarily causal relations between variants, highlighting Markovian and frequency-dependent properties of evolutionary processes, although they indicate that their use of a non-parametric transition matrix was not intended as an "adequate formal modelling tool" ([5], p.7). Our transition matrix (Equation 7) exhibits relatively high values along the leading diagonal, which is consistent with "homo-impact" [5], such that the frequency of variants are more strongly affected by their own prior frequency than by others', such as caused by imitation. But our diagonal values are higher for the granny knots than for the reef knots, and indeed the reef knot diagonal values are not dissimilar to the off-diagonal elements; this is consistent with what Cladiere et al call "hetero-impact", or between-variant frequency-dependent effects such as caused by mirroring. These observations indicate that different factors may be affecting granny and reef knot frequencies. If these factors were variant-specific (e.g. a bias for either LL, RR, LR or RL), a non-parametric transition matrix would suffice, but our analysis suggests that cognitive factors affect learning of particular knot properties or relations, so it is best to employ a parametric approach to account for the non-linear interactions between these factors.

The use of ABC illustrates how cross-generation data can be used to estimate the influence of the proposed cognitive factors. The narrow posterior distributions and the matching of the posterior handedness estimate to the experiment stage one results are encouraging signals of their explanatory value but of course we cannot rule out the influence of other factors not considered in our model. Using our mathematical model of the cultural evolutionary dynamic, ABC has the obvious advantage over a generalized linear regression approach in that it accounts for non-linear interactions between cognitive factors as structured in the social learning process. Although we are estimating the effects of individual-level properties of learning by comparing simulated and observed population-level measures

of cultural variation, our task is made easier by having individual-level data; i.e. we know what each individual observed and which knot they tied.

We restricted our analysis to a small closed set of cultural variants so social learning errors, or mutations, are a source of population-level variation even though the mutation may often not be novel to the population. In the open set of knots collated by Ashley [22], knot variation is likely to be constrained by technical properties, social function and aesthetic qualities. Nonetheless, it is possible that the cognitive factors we have investigated may affect the distribution of pairs of trefoils within composite knots (i.e. microstructure). Of the composite knots within Ashley, the proportion of granny to reef knots exactly matches the 3 to 1 ratio predicted by our parametric model at equilibrium in the absence of non-random error and mirroring and is similar to that predicted using the posterior estimates from the experiment (approx. 81% granny knots) [22] [23]. We resist drawing strong conclusions from the similarity between our results and the single population-level estimate of granny and reef knot frequencies found in Ashley's corpus but the correlation indicates that our modelling treatments of the experimental sample may be worth developing further, for instance, to consider micro-structure variation that may be redundant in relation to function (i.e. synonymous mutation). Analysis of experimental and real-world data should allow us to unpick the cognitive, ecological and social factors affecting the evolution of cultural variation.

Appendix A. Questionnaire Information

As part of the experiment described in Section 2 the participants were asked to complete a questionnaire detailing their name, gender, degree programme, handedness and hand usually written with, their knot tying experience and whether they knew how to tie a reef or granny knot. The questionnaire was filled in by participants at the end of the experiment, when all materials had been collected.

Participants recorded the hand they usually write with.

		Trefoil Tied		
		Right	Left	Total
Hand usually written with	Right	25	62	87
	Left	4	6	10
Self reported handedness	Right	23	58	81
	Left	4	5	9
	Ambidextrous	2	5	7
	Total	29	68	97

Table 4. Handedness of trefoils tied given hand usually written with

The majority of participants usually wrote with their right hand and tied a majority of left trefoils. Using a Bayesian analysis to test proportions [30] shown in Figure 12 we see there is a larger probability of tying a left handed trefoil by participants who usually wrote with their right hand than those who wrote with their left. Similarly there is a larger probability of tying a right handed trefoil by those who usually wrote with their left hand. However, the percentage of participants who usually wrote with their left hand is quite low so might not be wholly representative. The same result can be found using the self reported handedness data with those reporting as ambidextrous having a larger probability of tying a left trefoil. However, as most of those reporting as ambidextrous usually wrote with their right hand, this fits with the test of proportions for hand written with and trefoil tied.

Participants were asked to record their gender in a free-form box.

		Tied correct knot		
		Y	N	Total
Gender	Male	19	17	36
	Female	28	33	61
	Other	2	1	3
	Total	49	51	100

Table 5. Performance in experiment given gender

Table 5 shows the proportion of participants who tied the knot shown in the video given their gender. It is clear to see that their gender had no bearing on their performance in the experiment.

Participants were asked to rate their experience in knot tying on a scale of one to five, with one meaning they considered themselves a beginner and five an expert. They then had the opportunity to give details in a free-form box.

		Tied correct knot		
		Y	N	Total
Experience	1	18	19	37
	2	10	11	21
	3	14	14	28
	4	7	6	13
	5	0	1	1
	Total	49	51	100

Table 6. Performance in experiment given knot tying experience

Table 6 shows the proportion of participants who tied the knot shown in the video given the experience rated on the questionnaire. It is clear to see that the self rated experience had no bearing on the performance in the experiment.

Participants were also asked whether they knew how to tie a granny and a reef knot.

		Knot tied		
		Granny	Reef	Total
Knew how to tie a granny knot	Yes	17	13	30
	No	45	25	70
	Total	62	38	100

Table 7. Performance in experiment given knowledge of granny knots

		Knot tied		
		Granny	Reef	Total
Knew how to tie a reef knot	Yes	17	17	34
	No	45	21	66
	Total	62	38	100

Table 8. Performance in experiment given knowledge of reef knots

Tables 7 and 8 show the proportion of participants who tied granny and reef knots given the knowledge rated on the questionnaire. It is clear to see that the

self rated knowledge also had no bearing on the knots tied in the experiment. It is interesting to note that more participants knew how to tie the reef knot than the granny. This could be due to the belief that the reef knot is superior to the granny and so more likely to be taught.

Appendix B. Posterior simulations

Posterior simulations of the test of proportions generated using R package Bayesian First Aid [31]. The test of proportions assumes flat priors constructed as a Beta(1,1) distribution.

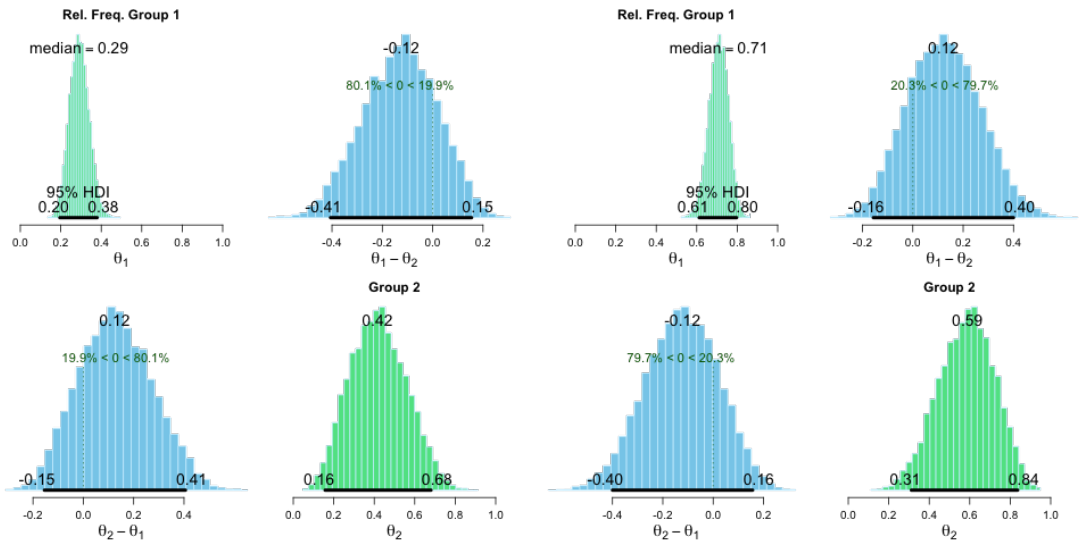

(A) Posterior simulation of right trefoils tied (B) Posterior simulation of left trefoils tied

Figure 12. Figure 12a shows the simulations of tying right handed trefoils by those who wrote with either hand. θ_1 refers to those who wrote with their right hand and tied a right trefoil whilst θ_2 refers to those who wrote with their left hand and tied a right trefoil, the differences $\theta_1 - \theta_2$ and $\theta_2 - \theta_1$ refer to the difference between these groups. We see there is a larger probability of those who write with their left hand tying a right handed trefoil than those who wrote with their right hand. Figure 12b shows the simulations of tying left handed trefoils by those who wrote with either hand. θ_1 refers to those who wrote with their right hand and tied a left trefoil whilst θ_2 refers to those who wrote with their left hand and tied a left trefoil, the differences $\theta_1 - \theta_2$ and $\theta_2 - \theta_1$ refer to the difference between these groups. We see there is a larger probability of those who write with their right hand tying a left handed trefoil than those who wrote with their left hand. However if we look at both Figures 12a and 12b we see those who wrote with their left hand were slightly more likely to tie a left handed trefoil than a right handed as the left handed trefoil was the most common amongst both groups and there were relatively few people reporting as writing with their left hand.

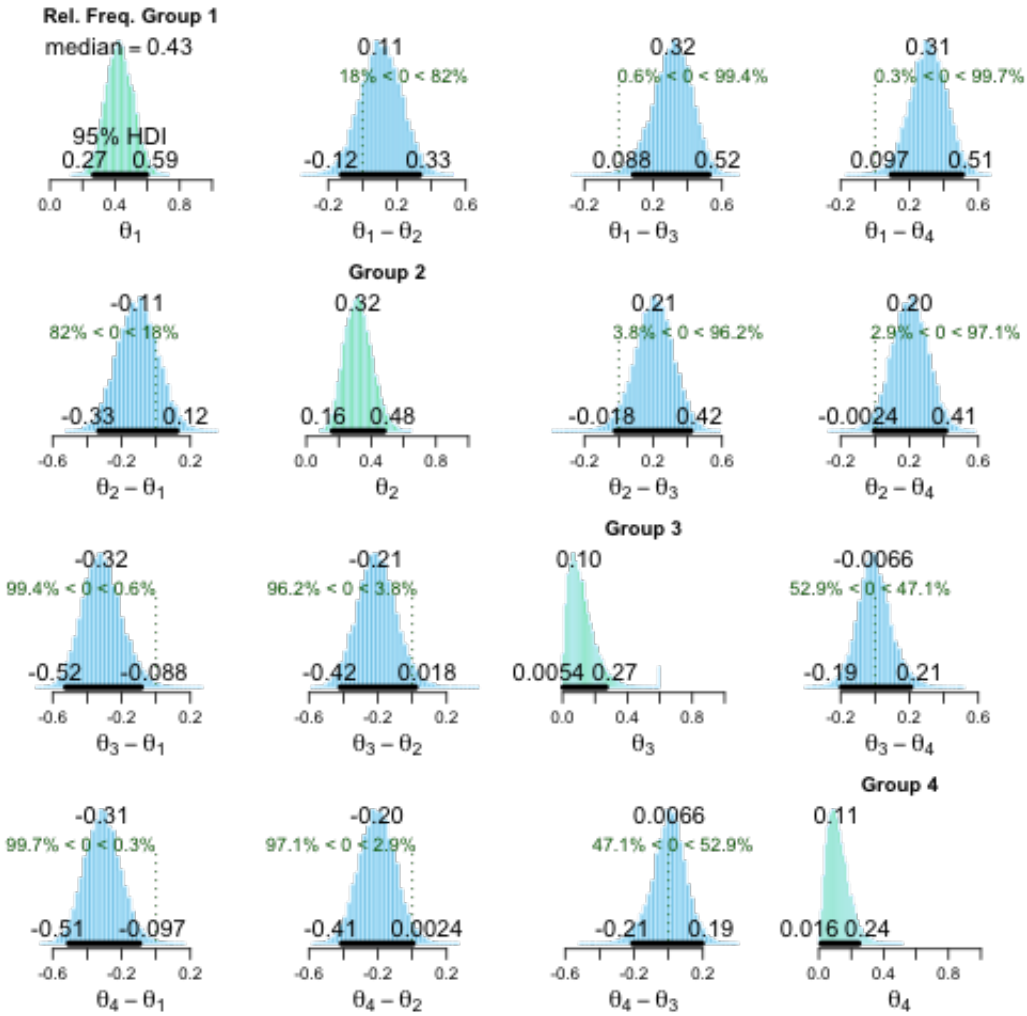

FIGURE 13. Posterior simulation of LL knots tied given demonstration knot. θ_1 refers to those who were shown the knot LL and tied LL, θ_2 those who were shown RR and tied LL, θ_3 those who were shown LR and tied LL and θ_4 those who were shown RL and tied LL with $\theta_i - \theta_j, (i, j \in \{1, 2, 3, 4\}, i \neq j)$ referring to the difference between groups. We see a larger probability for those who were shown either LL or RR tying LL than LR or RL, with those shown LL having the largest probability.

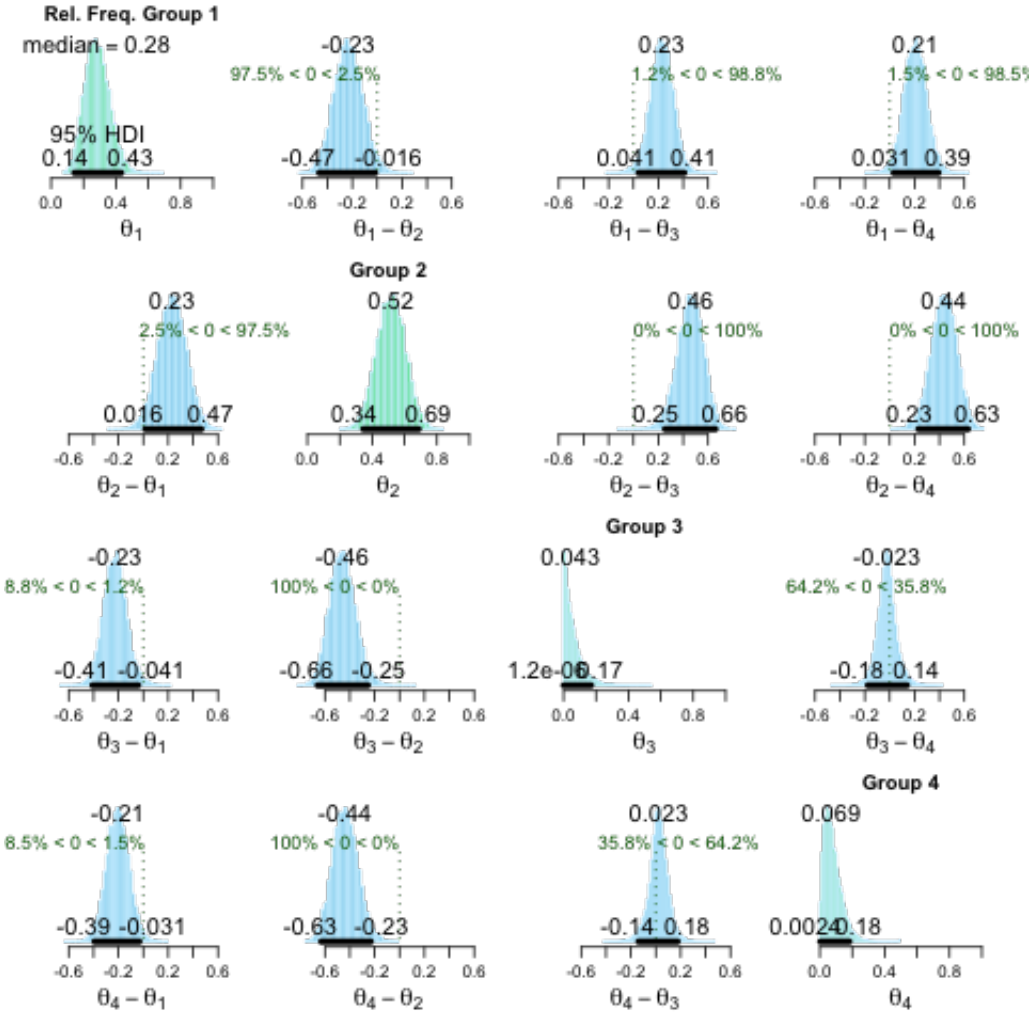

FIGURE 14. Posterior simulation of RR knots tied given demonstration knot. θ_1 refers to those who were shown the knot LL and tied RR, θ_2 those who were shown RR and tied RR, θ_3 those who were shown LR and tied RR and θ_4 those who were shown RL and tied RR with $\theta_i - \theta_j, (i, j \in \{1, 2, 3, 4\}, i \neq j)$ referring to the difference between groups. We see a larger probability for those who were shown either LL or RR tying RR than LR or RL, with those shown RR having the largest probability.

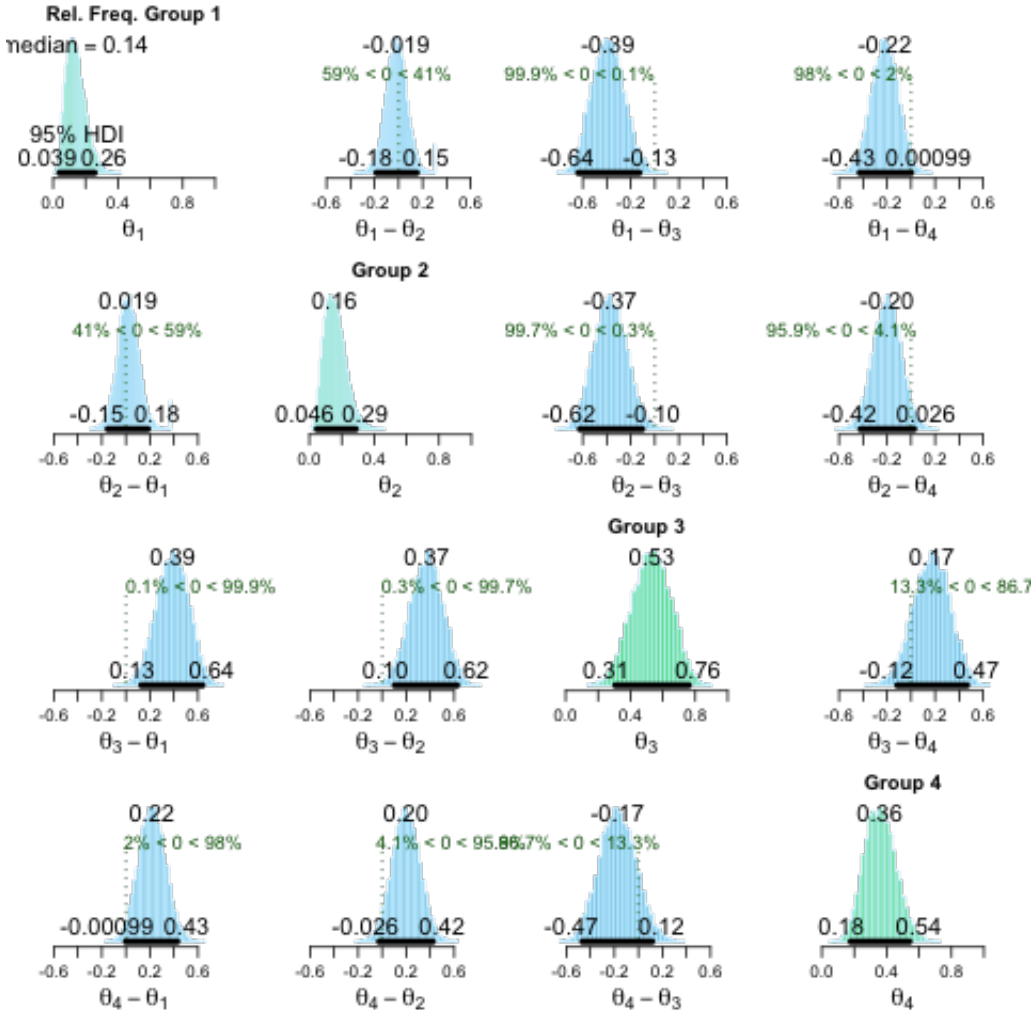

FIGURE 15. Posterior simulation of LR knots tied given demonstration knot. θ_1 refers to those who were shown the knot LL and tied LR, θ_2 those who were shown RR and tied LR, θ_3 those who were shown LR and tied LR and θ_4 those who were shown RL and tied LR with $\theta_i - \theta_j, (i, j \in \{1, 2, 3, 4\}, i \neq j)$ referring to the difference between groups. We see a larger probability for those who were shown either LR or RL tying LR than LL or RR, with those shown LR having the largest probability.

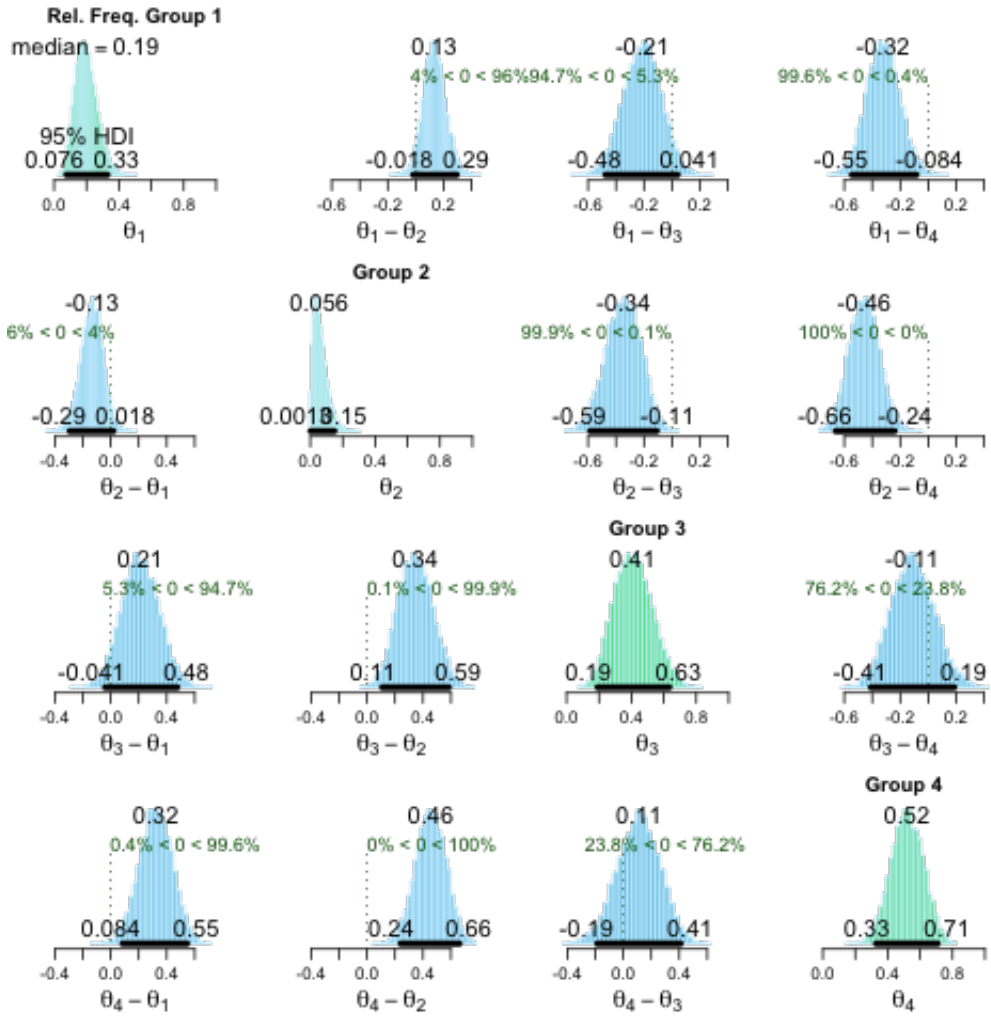

FIGURE 16. Posterior simulation of RL knots tied given demonstration knot. θ_1 refers to those who were shown the knot LL and tied RL, θ_2 those who were shown RR and tied RL, θ_3 those who were shown LR and tied RL and θ_4 those who were shown RL and tied RL with $\theta_i - \theta_j, (i, j \in \{1, 2, 3, 4\}, i \neq j)$ referring to the difference between groups. We see a larger probability for those who were shown either LR or RL tying RL than LL or RR, with those shown RL having the largest probability.

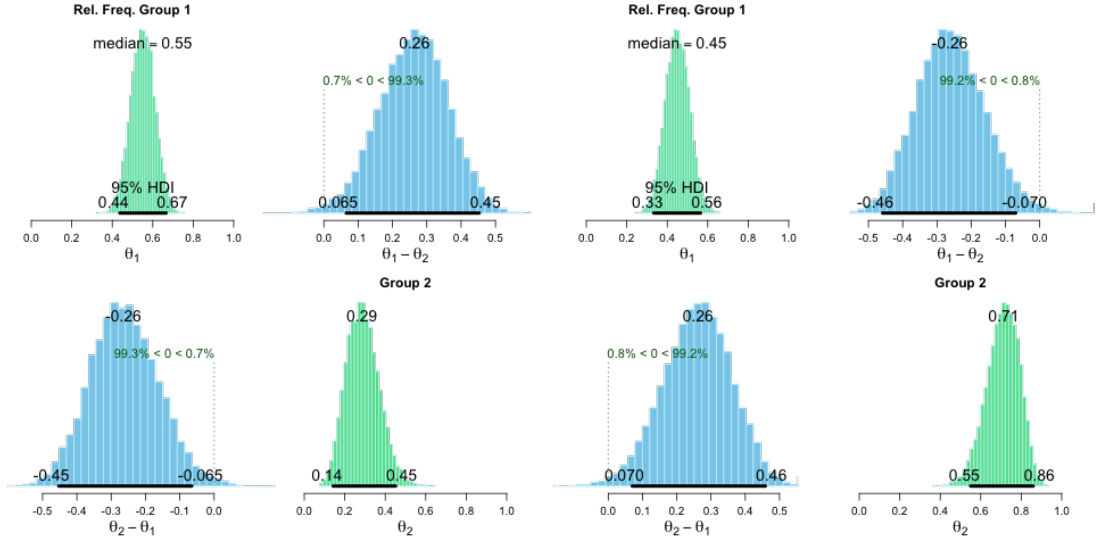

(A) Posterior simulation of knots tied by those with a left hand bias in stage 1

(B) Posterior simulation of knots tied by those with a right hand bias in stage 1

FIGURE 17. Figure 17a shows the simulations of tying an L or R knot first post demonstration given a left hand bias in stage 1. θ_1 refers to those who had a left hand bias in stage 1 and tied an L knot first post demonstration, θ_2 those who had a left hand bias and tied an R knot first and $\theta_1 - \theta_2$ and $\theta_2 - \theta_1$ the difference between groups. We see there is a larger probability of those who had a left hand bias starting their post-demonstration knot with an L knot than an R. Figure 17b shows the simulations of tying an L or R knot first post demonstration given a right hand bias in stage 1. θ_1 refers to those who had a right hand bias in stage 1 and tied an L knot first post demonstration, θ_2 those who had a right hand bias and tied an R knot first and $\theta_1 - \theta_2$ and $\theta_2 - \theta_1$ the difference between groups. We see there is a larger probability of those who had a right hand bias starting their post-demonstration knot with an R knot than an L.

Appendix C. Equations

The equations are

$$
\begin{aligned}
f'_{RR} =& f_{RR}((1-g)s^2 + (1-s)^2(1-r)p^2 + (1-s)^2rp + 2(1-g)s(1-s)r) \\
&+2(1-g)s(1-s)(1-r)p \\
&+f_{LL}((1-s)^2(1-r)p^2 + (1-s)^2rp + gs^2 + 2gs(1-s)r) \\
&+2gs(1-s)(1-r)p \\
&+(f_{RL} + f_{LR})((1-s)^2(1-r)p^2 + (1-s)^2rp + s(1-s)r \\
&+s(1-s)(1-r)p)
\end{aligned} \tag{8}
$$

$$
\begin{aligned}
f'_{LL} =& f_{RR}(gs^2 + (1-s)^2(1-r)(1-p)^2 + (1-s)^2r(1-p) + 2gs(1-s)r \\
&+2gs(1-s)(1-r)(1-p)) \\
&+f_{LL}((1-g)s^2 + (1-s)^2(1-r)(1-p)^2 + (1-s)^2r(1-p) \\
&+2(1-g)s(1-s)(1-r)(1-p) + 2(1-g)s(1-s)r) \\
&+(f_{RL} + f_{LR})((1-s)^2(1-r)(1-p)^2 + (1-s)^2r(1-p) \\
&+s(1-s)(1-r)(1-p) + s(1-s)r)
\end{aligned} \tag{9}
$$

$$
\begin{aligned}
f'_{RL} =& f_{RR}((1-s)^2(1-r)p(1-p) + (1-g)s(1-s)(1-r)(1-p) \\
&+g(1-s)s(1-r)p) \\
&+f_{LL}((1-s)^2(1-r)p(1-p) + (1-g)(1-s)s(1-r)p \\
&+gs(1-s)(1-r)(1-p)) \\
&+f_{RL}((1-g)s^2 + (1-s)^2(1-r)p(1-p) + (1-g)s(1-s)(1-r)) \\
&+f_{LR}(gs^2 + (1-s)^2(1-r)p(1-p) + gs(1-s)(1-r))
\end{aligned} \tag{10}
$$

$$
\begin{aligned}
f'_{LR} =& f_{RR}((1-s)^2(1-r)(1-p)p + (1-g)(1-s)s(1-r)(1-p) \\
&+gs(1-s)(1-r)p) \\
&+f_{LL}((1-s)^2(1-r)(1-p)p + (1-g)s(1-s)(1-r)p \\
&+g(1-s)s(1-r)(1-p)) \\
&+f_{RL}(gs^2 + (1-s)^2(1-r)(1-p)p + gs(1-s)(1-r)) \\
&+f_{LR}((1-g)s^2 + (1-s)^2(1-r)(1-p)p + (1-g)s(1-s)(1-r))
\end{aligned} \tag{11}
$$

Appendix D. Equilibria Equations

Equilibria occur when

$$\hat{f}_{RR} = \frac{Q_1}{P}$$

where

(12)

$$\begin{aligned} Q_1 = &-p^2(r-1)(s-1)(1+s(2g-1)(r-1)+rs^2(2g-1)) + gs(r(s^2-2)-s) \\ &+ p(s-1)(2gs + r^2s(2g-1)(1+s) + r(1+s-2gs(2-s))) \end{aligned}$$

$$\hat{f}_{LL} = \frac{Q_2}{P}$$

where

$$\begin{aligned} Q_2 = &\, s^2(1-g) - p^2(r-1)(s-1)(1+s(2g-1)(r-1)+rs^2(2g-1)) - 1 \\ &+ r(s(1-2g)+s^3(g-1)) + p(s-1)(r^2s(2g-1)(1+s) \\ &+ 2s(g-1) + rs(1+(3-4g)-2s^2(g-1)) - 2) \end{aligned} \tag{13}$$

$$\hat{f}_{LR} = \frac{Q_3}{P}$$

where

$$Q_3 = (r-1)(gs - p(s-1)(1+p^2(s-1))(1+(2g-1)(s(r-1)+rs^2))) \tag{14}$$

$$\hat{f}_{RL} = \frac{Q_4}{P}$$

where

$$Q_4 = (r-1)(gs - p(s-1)(1+p^2(s-1))(1+(2g-1)(s(r-1)+rs^2))) \tag{15}$$

and

$$P = (1+s)(s(2g-1)(rs-r-1)-1). \tag{16}$$

Appendix E. Stability

In this system, an equilibrium point is stable if no matter the starting values of f_{RR}, f_{LL}, f_{LR}, f_{RL}, the system comes to rest at the same point. If the point changes depending on these starting values then it is not stable.

To find the stable equilibrium points we set f_{ij} equal to the equilibria points determined by the equations, plus some small perturbation ϵ_{ij}. The equilibrium is stable if the value of f'_{ij}, moves towards the equilibria points given by the equations in Appendix D.

Let

$$f_{RR} = \frac{Q_1}{P} + \epsilon_{RR} \tag{17}$$

$$f_{LL} = \frac{Q_2}{P} + \epsilon_{LL} \tag{18}$$

$$f_{LR} = \frac{Q_3}{P} + \epsilon_{LR} \tag{19}$$

$$f_{RL} = \frac{Q_4}{P} + \epsilon_{RL} \tag{20}$$

where Q_i and P are as given in Appendix D, and

$$\epsilon_{RL} = -\epsilon_{RR} - \epsilon_{LL} - \epsilon_{LR} \tag{21}$$

to ensure f_{ij} sum to one.

We then compute f'_{RR}, f'_{LL}, f'_{LR}, f'_{RL} and the distance:

$$d_{RR} = f'_{RR} - \frac{Q_1}{P} \tag{22}$$

$$d_{LL} = f'_{LL} - \frac{Q_2}{P} \tag{23}$$

$$d_{LR} = f'_{LR} - \frac{Q_3}{P} \tag{24}$$

$$d_{RL} = f'_{RL} - \frac{Q_4}{P} \tag{25}$$

We then have the following cases.

Case 1:

$$d_{ij} = 0 \tag{26}$$

In this case the system jumps to an equilibrium point given by the parameters. The system then remains at this point for all generations. This occurs when there

is no accurate imitation, when $s = 0$. The system is not affected by starting values of f_{ij}, the frequency of each type of knot is determined solely by the values of p and r.

Case 2:

$$d_{ij} = \epsilon_{ij} \tag{27}$$

In this case there is no change in the system, meaning the system is currently at equilibria, with the system remaining at this point for all generations. This occurs when imitation is always accurate and mirroring never occurs, when $s = 1$ and $g = 0$. The equilibrium state is determined by the starting values of f_{ij} and is independent of the values of p and r. The frequency of each type of knot remains constant across generations.

Case 3:

$$d_{ij} < \epsilon_{ij} \tag{28}$$

In this case the system moves towards the equilibrium point given by the parameters. This occurs when $s < 1$, when imitation is not perfect and the system evolves towards equilibria over generations.

Case 4:

$$d_{ij} > \epsilon_{ij} \tag{29}$$

In this case the system moves away from the equilibrium point given by the parameters. This never occurs for any equilibrium point in the system, meaning all points are stable.

Appendix F. Barycentric Coordinates

We plot a tetrahedron with vertices at the points $\begin{pmatrix}1\\0\\0\end{pmatrix}$, $\begin{pmatrix}0\\1\\0\end{pmatrix}$, $\begin{pmatrix}0\\0\\1\end{pmatrix}$ and $\begin{pmatrix}1\\1\\1\end{pmatrix}$.

Taking values of f'_{ij} from our equations, we can represent the values of f'_{ij} as points $\mathbf{p}$ inside the tetrahedron using the conversion

$$\mathbf{p} = \begin{pmatrix} f'_{RR} + f'_{RL} \\ f'_{LL} + f'_{RL} \\ f'_{LR} + f'_{RL} \end{pmatrix} \tag{30}$$

References

[1] H. M. Lewis and K. N. Laland, "Transmission fidelity is the key to the build-up of cumulative culture," *Philos. Trans. R. Soc. B Biol. Sci.*, vol. 367, no. 1599, pp. 2171–2180, aug 2012.

[2] M. Muthukrishna, B. W. Shulman, V. Vasilescu, and J. Henrich, "Sociality influences cultural complexity." *Proc. Biol. Sci.*, vol. 281, p. 20132511, 2014.

[3] A. Mesoudi, *Cultural evolution: How Darwinian theory can explain human culture and synthesize the social sciences.* Chicago, IL: University of Chicago Press, 2011.

[4] J. W. Eerkens and C. P. Lipo, "Cultural transmission, copying errors, and the generation of variation in material culture and the archaeological record," *J. Anthr. Archaeol.*, vol. 24, no. 4, pp. 316–334, 2005.

[5] N. Claidière, T. C. Scott-phillips, and D. Sperber, "How Darwinian is cultural evolution?" *Philos. Trans. R. Soc. B Biol. Sci.*, no. March, 2014.

[6] M. Kempe, S. Lycett, and A. Mesoudi, "An Experimental Test of the Accumulated Copying Error Model of Cultural Mutation for Acheulean Handaxe Size," *PLoS One*, vol. 7, no. 11, 2012.

[7] K. Schillinger, A. Mesoudi, and S. J. Lycett, "Copying error and the cultural evolution of additive vs. reductive material traditions: An experimental assessment," *American Antiquity*, vol. 79, no. 1, p. 128143, 2014.

[8] A. Wohlschläger, M. Gattis, and H. Bekkering, "Action generation and action perception in imitation: an instance of the ideomotor principle." *Philos. Trans. R. Soc. Lond. B. Biol. Sci.*, vol. 358, no. 1431, pp. 501–515, 2003.

[9] C. Chiavarino, I. A. Apperly, and G. W. Humphreys, "Exploring the functional and anatomical bases of mirror-image and anatomical imitation: The role of the frontal lobes," *Neuropsychologia*, vol. 45, no. 4, pp. 784–795, 2007.

[10] C. L. Nehaniv and K. Dautenhahn, "The Correspondence Problem," in *Imitation Anim. artifacts.* MIT Press, 2002, pp. 41–61.

[11] C. Heyes and G. Bird, "Mirroring, association, and the correspondence problem," *Sensorimotor Found. High. Cogn.*, pp. 461–480, 2007.

[12] K. Smith, "Learning bias, cultural evolution of language, and the biological evolution of the language faculty." *Hum. Biol.*, vol. 83, no. 2, pp. 261–278, 2011.

[13] O. Morin, "How portraits turned their eyes upon us: Visual preferences and demographic change in cultural evolution," *Evol. Hum. Behav.*, vol. 34, no. 3, pp. 222–229, may 2013.

[14] J. Stubbersfield and J. Tehrani, "Expect the Unexpected? Testing for Minimally Counterintuitive (MCI) Bias in the Transmission of Contemporary Legends: A Computational Phylogenetic Approach," *Soc. Sci. Comput. Rev.*, vol. 31, no. 1, pp. 90–102, feb 2013.

[15] L. L. Cavalli-Sforza and M. W. Feldman, *Cultural Transmission and Evolution: A Quantitative Approach.* Princeton University Press, 1981.

[16] R. Boyd and P. J. Richerson, "Culture and the evolutionary process," p. 331, 1985.

[17] D. Sperber, *Explaining culture : a naturalistic approach.* Blackwell, 1996.

[18] A. Buskell, "What are cultural attractors?" *Biology & Philosophy*, vol. 32, no. 3, pp. 377–394, Jun 2017. [Online]. Available: https://doi.org/10.1007/s10539-017-9570-6

[19] J. Fonollosa, E. Neftci, and M. Rabinovich, "Learning of chunking sequences in cognition and behavior," *PLOS Computational Biology*, vol. 11, no. 11, pp. 1–24, 11 2015. [Online]. Available: https://doi.org/10.1371/journal.pcbi.1004592

[20] C. Warner and R. G. Bednarik, "Pleistocene Knotting," in *Hist. Sci. Knots*, P. C. Turner, J.C. Van de Griend, Ed. World Scientific, 1998, pp. 3–18.

[21] G. van der Kleij, "On Knots and Swamps: Knots in European Prehistory," in *Hist. Sci. Knots*, P. C. Turner, J.C. Van de Griend, Ed. World Scientific, 1998, pp. 31–42.

[22] C. W. Ashley, *Ashley Book of Knots.* Faber and Faber Limited, 1993.
[23] L. A. Scanlon, "Study of knots in material culture," *J. Knot Theory Ramifications*, vol. 25, no. 9, 2016.
[24] Grog, "Animated Knots Reef Knot — How to tie the Reef Knot — The Basics Knots." [Online]. Available: http://www.animatedknots.com/reef/
[25] O. M. O'reilly, C. A. Daily-Diamond, and C. E. Gregg, "The roles of impact and inertia in the failure of a shoelace knot," *Proc. R. Soc. A Math. Phys. Eng. Sci.*, 2017.
[26] K. Reidemeister, "Elementare Begründung der Knotentheorie," *Abhandlungen aus dem Math. Semin. der Univ. Hambg.*, vol. 5, no. 1, pp. 24–32, dec 1927.
[27] C. C. Adams, *The Knot Book: An Elementary Introduction to the Mathematical Theory of Knots.* American Mathematical Soc., 2004.
[28] V. F. R. Jones, "A polynomial invariant for knots via Von Neumann algebras," *Bull. Am. Math. Soc.*, vol. 12, no. 1, pp. 103–111, 1985.
[29] M. Sunnåker, A. G. Busetto, E. Numminen, J. Corander, M. Foll, and C. Dessimoz, "Approximate Bayesian Computation," *PLoS Comput. Biol.*, vol. 9, no. 1, p. e1002803, jan 2013.
[30] A. Gelman, J. B. Carlin, H. S. Stern, and D. B. Rubin, *Bayesian Data Analysis*, 3rd ed. Chapman and Hall/CRC, 2003, vol. 2.
[31] R. Bååth, "Bayesian First Aid: A Package that Implements Bayesian Alternatives to the Classical * .test Functions in R," in *UseR! 2014 - Int. R User Conf.*, 2014.